Article

Discovery Medicine 2026; 38(206): 892–905
https://doi.org/10.24976/Discov.Med.202638206.73

HDAC6-PRKN-KEAP1 Cascade Regulates Kainic Acid-Induced Ferroptosis and Neuroinflammation in HT22 Hippocampal Neurons

Junwei He[1,*,†], Tianyang Wu[2,†], Yukun Lin[3], Yipan Zhang[1]

[1]Department of Neurology, The Affiliated Hospital of Putian University, 351100 Putian, Fujian, China
[2]Department of Neurosurgery, The First Affiliated Hospital of Bengbu Medical university, 233000 Bengbu, Anhui, China
[3]Department of Rehabilitation Medicine, The Affiliated Hospital of Putian University, 351100 Putian, Fujian, China
*Correspondence: ga2008medy@163.com (Junwei He)
[†]These authors contributed equally.
Submitted: 16 December 2025 Revised: 29 January 2026 Accepted: 3 March 2026 Published: 20 March 2026

Background: Ferroptosis has emerged as a pivotal mechanism in epilepsy development. Kelch-like ECH-associated protein 1 (KEAP1), a critical regulator of the nuclear factor erythroid 2-related factor 2 (NRF2) pathway, plays a pivotal role in oxidative stress and is implicated in seizure recurrence. This study aimed to elucidate the mechanistic role of KEAP1 in kainic acid (KA)-induced ferroptosis and neuroinflammation.

Methods: HT22 hippocampal neuronal cells were stimulated with KA to establish the *in vitro* excitotoxicity model. Cell viability and apoptosis were detected using 3-(4,5-dimethylthiazol-2-yl)-2,5-diphenyltetrazolium bromide (MTT) assay and flow cytometry, respectively. Inflammatory responses were evaluated by detecting interleukin 6 (IL-6) and tumor necrosis factor alpha (TNF-α) secretion levels. Ferroptosis was evaluated by measuring Fe^{2+}, glutathione (GSH), and reactive oxygen species (ROS) levels. The parkin RBR E3 ubiquitin protein ligase (PRKN)-KEAP1 and histone deacetylase 6 (HDAC6)-PRKN interactions were assessed by co-immunoprecipitation (Co-IP) experiments.

Results: KEAP1 ($p = 0.0008$) and HDAC6 ($p = 0.0004$) protein levels were upregulated in the KA-induced HT22 cells, while PRKN expression was downregulated ($p = 0.0034$). Knockdown of KEAP1 alleviated KA-induced neuroinflammation by reducing the secretion of IL-6 ($p = 0.0021$) and TNF-α ($p = 0.0003$). Furthermore, it suppressed ferroptosis, as demonstrated by decreased levels of Fe^{2+} ($p = 0.0022$) and ROS ($p < 0.01$), and an increased GSH content ($p = 0.0057$). In addition, KEAP1 silencing attenuated apoptosis ($p = 0.0016$) in KA-induced cells. Mechanistically, PRKN mediated KEAP1 ubiquitination and degradation ($p = 0.0054$); HDAC6 induced PRKN deacetylation ($p < 0.001$), and HDAC6 modulated KEAP1 expression via PRKN. In KA-treated HT22 cells, KEAP1 reconstitution counteracted PRKN overexpression-mediated anti-inflammatory and ferroptosis-inhibitory effects ($p < 0.05$), while PRKN knockdown reversed the protective effects conferred by HDAC6 silencing ($p < 0.05$). Additionally, PRKN regulated the NRF2/solute carrier family 7 member 11 (SLC7A11)/glutathione peroxidase 4 (GPX4) pathway through KEAP1 ($p < 0.05$).

Conclusion: Our study uncovers a novel HDAC6-PRKN-KEAP1 cascade that critically modulates KA-induced ferroptosis and neuroinflammation in HT22 neuronal cells.

Keywords: epilepsy; hippocampal neuron; KEAP1; ubiquitination; protein deacetylation

Introduction

Epilepsy, a chronic neurological disorder characterized by recurrent, unprovoked seizures, affects over 50 million individuals globally and imposes a significant burden on cognitive function, mental health, and quality of life [1]. Emerging evidence highlights the critical roles of neuroinflammation and oxidative stress in epileptogenesis, contributing to neuronal hyperexcitability, synaptic dysfunction, and neuronal death [2,3]. In particular, hippocampal neurons undergo significant changes in epilepsy, including neuronal loss, axonal sprouting, and altered excitatory-inhibitory balance, which are closely associated with seizure activity and cognitive dysfunction [4]. Ferroptosis, a recently identified iron-dependent form of regulated cell death, has emerged as a pivotal mechanism underlying neurodegenerative and neuroinflammatory disorders [5,6]. Pharmacological inhibition of ferroptosis has shown to attenuate seizure severity and alleviate hippocampal damage [7]. These findings underscore ferroptosis as a novel therapeutic target for modulating neuronal injuries.

Kelch-like ECH-associated protein 1 (KEAP1), a critical redox-sensitive regulator of the nuclear factor erythroid 2-related factor 2 (NRF2)/antioxidant response element (ARE) pathway, functions as a substrate adaptor for the

Cullin3 ubiquitin ligase complex, leading to NRF2 degradation under basal conditions. Under oxidative or electrophilic stress, KEAP1 undergoes covalent modification, leading to NRF2 stabilization and nuclear translocation, and activates the transcription of cytoprotective genes [8]. Dysregulation of the KEAP1/NRF2 axis has been implicated in diverse pathologies, including vascular diseases, cancer, and neurodegenerative disorders, where altered KEAP1 expression or mutations either exacerbate oxidative damage or promote disease progression [9–11]. Inhibition of KEAP1 activates NRF2 to reduce oxidative stress and mitochondrial dysfunction, thereby suppressing epilepsy development [12]. The KEAP1/NRF2/ARE/heme oxygenase 1 (HO-1) axis represents a promising neuroprotective target [13]. However, the mechanistic role of KEAP1 in kainic acid (KA)-induced neuronal ferroptosis remains poorly understood.

PRKN (parkin RBR E3 ubiquitin protein ligase), an E3 ubiquitin ligase, plays a pivotal role in regulating ubiquitin-proteasome system and in mitochondrial quality control [14]. Recent studies highlight its neuroprotective functions in neurodegenerative disorders, where PRKN downregulation exacerbates neuronal damage by impairing mitochondrial homeostasis and increasing oxidative stress [15]. Notably, PRKN has been specifically implicated in regulating the NRF2 pathway and inhibiting ferroptosis through acyl-CoA synthetase long-chain family member 1 (ACSL1) ubiquitination, suggesting a broader function in cellular stress responses [16]. Histone deacetylase 6 (HDAC6), a cytosolic enzyme, regulates protein deacetylation and aggregation clearance [17]. In epilepsy, altered HDAC6 expression contributes to disease pathophysiology by modulating cytoplasmic substrates and neurotransmitter receptor expression [18]. Inhibition of HDAC6 promotes neuronal survival and synaptic defects in cyclin-dependent kinase-like 5 (CDKL5) deficiency disorder, demonstrating therapeutic potential for HDAC6-targeted approaches in developmental epilepsies [19]. Importantly, HDAC6 activity has been linked to the modulation of ferroptosis in a neurodegenerative disorder [20]. Therefore, given their established roles in mitigating oxidative stress and ferroptosis, PRKN and HDAC6 were prioritized for further investigation to explore their potential interaction and synergistic effects in our experimental model.

This study established a KA-induced HT22 neuronal injury model, revealing that KEAP1 upregulation contributes to neuroinflammation and ferroptosis. Our study further demonstrated a novel HDAC6-PRKN-KEAP1 cascade that critically modulates HT22 neuronal cytotoxicity induced by KA. We provide novel evidence that coordinated post-translational modifications (ubiquitination and deacetylation) play pivotal roles in neurotoxicity.

Materials and Methods

Cell Culture and Treatment

In this study, an immortalized mouse hippocampal neuron HT22 cell line (Catalog #IM-M038, Immocell, Xiamen, China) and primary mouse hippocampal neurons (Catalog #CP-M107, Procell, Wuhan, China) were used. HT22 cells were authenticated using short tandem repeat (STR) profiling and confirmed to be free of mycoplasma contamination by periodic testing using a PCR-based detection assay. The primary mouse hippocampal neurons exhibited rounded soma with extended, branched neurites, characteristic of neuronal morphology. As certified by the commercial vendor (Procell), the cells were identified via β-Tubulin-III immunofluorescence with a purity of over 90%. Furthermore, the cells were verified to be negative for HIV-1, HBV, HCV, mycoplasma, and other common microbiological contaminants such as bacteria, yeast, and fungi. Neuronal cells were maintained at 37 °C in complete growth medium composed of 89% (v/v) Dulbecco's Modified Eagle Medium (DMEM, Catalog #C11995500BT, Gibco, Schwerte, Germany), 10% (v/v) fetal bovine serum (FBS, Catalog #10099141C, Gibco), and 1% penicillin/streptomycin (Catalog #P4333, Beyotime, Shanghai, China) in a humidified 5% CO_2 incubator (Model #3111, Thermo Fisher Scientific, Saint-Aubin, France). To establish an *in vitro* neurotoxicity model, HT22 cells were stimulated with KA (Catalog #ab120100, Abcam, Cambridge, UK, purity: >99%) at a concentration of 100 µM for 12 h as previously described [21]. Additionally, HT22 neurons were exposed to 1 µM Ferrostatin-1 (a selective ferroptosis inhibitor, Catalog #SML0583, Sigma-Aldrich, St. Louis, MO, USA) [22], 10 µM Erastin (a ferroptosis inducer, Catalog #E7781, Sigma-Aldrich) [23], or 50 µM MG132 (a proteasome inhibitor, Catalog #S2619, Selleckchem, Houston, TX, USA) [24] for 12 h for different experimental purposes.

SiRNAs, Plasmids, and Transfection of Cell Line

The pCMV-PRKN(mouse)-Flag-Neo (Catalog #P82298, OE-PRKN), pCMV-KEAP1(mouse)-mCherry-Puro (Catalog #P81647, OE-KEAP1), and corresponding control (Catalog #P0860, OE-NC) plasmids were procured from Miaoling Plasmid (Wuhan, China). The small interfering RNA (siRNA) pools (MedChemExpress, Shanghai, China) used in this study included KEAP1 Mouse Pre-designed siRNA Set A (Catalog #HY-RS07231, si-KEAP1), HDAC6 Mouse Pre-designed siRNA Set A (Catalog #HY-RS06080, si-HDAC6), and PRKN Mouse Pre-designed siRNA Set A (Catalog #HY-RS18966, si-PRKN), with the nontarget siRNA (Catalog #HY-150150, si-NC) as the control. Each siRNA pool consisted of three distinct duplexes targeting different regions of the mouse "KEAP1", "HDAC6" or "PRKN" transcript, thereby significantly reducing the risk of off-target effects. The

sequence information of siRNAs/plasmids was shown in **Supplementary Table 1**.

In accordance with the manufacturer's guidelines, the transient transfection of siRNA or/and plasmid into neurons was conducted using Lipofectamine 3000 (Catalog #L3000150, Thermo Fisher Scientific). Briefly, for each well of a 6-well plate, siRNA (final concentration 50 nM) or plasmid DNA (2.5 µg) was diluted in 125 µL of Opti-MEM reduced serum medium. Separately, 5 µL of Lipofectamine 3000 reagent was diluted in 125 µL of Opti-MEM. After 5-min incubation at room temperature, the diluted DNA/siRNA was combined with the diluted Lipofectamine 3000 reagent, mixed gently, and incubated for 15 min at room temperature to allow complex formation. The resulting transfection complexes were then added dropwise to the cultured neurons. After 6 h, the transfection medium was refreshed, followed by a 24–48 h incubation period prior to subsequent experiments, including KA induction or other assays.

Immunoblot Analysis

Protein samples were obtained from cultured HT22 neurons through lysis in Radioimmunoprecipitation assay buffer (RIPA) buffer (Catalog #P0013B, Beyotime) supplemented with added protease and phosphatase inhibitor cocktails (Catalog #P8340, Sigma-Aldrich). Quantified protein samples (25 µg per lane) were resolved by sodium dodecyl sulfate-polyacrylamide gel electrophoresis (SDS-PAGE) and transferred electrophoretically onto polyvinylidene fluoride (PVDF) membranes (Catalog #IPVH00010, Immobilon-P, Millipore, Burlington, MA, USA). Immunoblotting was performed using specific primary antibodies against KEAP1 (Catalog #ab119403, Abcam, 1:1500), PRKN (Catalog #ab77924, Abcam, 1:2000), ubiquitin (Ub, Catalog #3936, Cell Signaling Technology, Danvers, MA, USA, 1:1000), HDAC6 (Catalog #ab239362, Abcam, 1:1000), Acetylated-lysine (Ac-lysine, Catalog #ab190479, Abcam, 1:2000), NRF2 (Catalog #12721, CST, 1:1000), solute carrier family 7 member 11 (SLC7A11, Catalog #ab307601, Abcam, 1:1000), glutathione peroxidase 4 (GPX4, Catalog #ab231174, Abcam, 1:1000), and glyceraldehyde-3-phosphate dehydrogenase (GAPDH, Catalog #2118, CST, 1:1000), followed by incubation with horseradish peroxidase (HRP)-labeled secondary antibodies (Goat Anti-Rabbit IgG, Catalog #7074S, CST, 1:2000 or Goat Anti-Mouse IgG, Catalog #7076S, CST, 1:2000). Protein band intensities were quantified using a Chemi-Doc XRS+ imaging system (Model #1708265, Bio-Rad, Gladesville, NSW, Australia) and ImageJ (Version 1.53t, National Institutes of Health, Bethesda, MD, USA) for densitometric analysis. The intensity of each target protein band was normalized to the corresponding loading control band (GAPDH) from the same lane to calculate relative protein expression levels. These values were subsequently expressed as a fold change relative to the control group.

3-(4,5-Dimethylthiazol-2-yl)-2,5-Diphenyltetrazolium Bromide (MTT) Cell Viability Assay

Neuronal viability in HT22 cells was evaluated following transfection and/or KA exposure using the standard MTT assay (Catalog #C0009S, Beyotime). Briefly, 20 µL of 5 mg/mL MTT solution was added to each well, followed by 4-h incubation at 37 °C. After removing the supernatant, 150 µL dimethyl sulfoxide (DMSO, Catalog #D2650, Sigma-Aldrich) was introduced to solubilize the formazan precipitates. Following 15 min of gentle agitation, absorbance measurements were taken at 490 nm using the Infinite® M200 PRO reader (Tecan, Männedorf, Switzerland). Although the kit manufacturer recommends measuring absorbance at 570 nm, we used 490 nm as the detection wavelength based on established protocols in our laboratory. This wavelength has been validated for reliable formazan quantification in HT22 cells under our experimental conditions. This adjustment has been consistently applied in our assays and does not affect the comparative assessment of cell viability. Cell viability was calculated as a percentage relative to the control group using the formula: (Mean absorbance of treatment group / Mean absorbance of control group) $\times$ 100%.

Cell Apoptosis Assay

Apoptosis was evaluated in transfected and/or KA-treated HT22 cells using an Annexin V-fluorescein isothiocyanate (FITC)/propidium iodide (PI) Staining Kit (Catalog #556547, BD Biosciences, Heidelberg, Germany) according to the manufacturer's instructions. Briefly, cells were collected, washed twice with cold PBS, and resuspended in 1$\times$ binding buffer at a concentration of 1 $\times$ 10^6 cells/mL. Subsequently, 100 µL of the cell suspension was incubated with 5 µL of Annexin V-FITC and 5 µL of PI in the dark at room temperature for 15 min. Cell staining was performed according to standardized procedures, with subsequent flow cytometric analysis conducted within 60 min using an LSRII system (BD Biosciences) to quantify apoptotic populations. Apoptosis rate was calculated as the percentage of cells in both early (Annexin V+/PI-) and late (Annexin V+/PI+) apoptotic quadrants relative to the total cell population.

Determination of Interleukin 6 (IL-6) and Tumor Necrosis Factor Alpha (TNF-α) Levels

Culture supernatants from transfected and/or KA-stimulated HT22 cells were analyzed for inflammatory cytokine secretion. IL-6 contents were determined with a commercial Mouse IL-6 enzyme-linked immunosorbent assay (ELISA) kit (Catalog #IC50325-1, Enzyme-linked Biotechnology, Shanghai, China), while TNF-α levels were measured with a Mouse TNF-α ELISA Kit (Catalog #ml002098, Enzyme-linked Biotechnology), both performed according to standardized protocols. Briefly,

collected supernatants were centrifuged to remove debris. Standards and samples were added to the antibody-precoated wells and incubated. After washing, biotinylated detection antibody was added, followed by incubation with streptavidin-HRP. Tetramethylbenzidine (TMB) substrate was added for color development, and the reaction was stopped with the stop solution. Cytokine concentrations were calculated by interpolating absorbance values (450 nm) against a standard curve generated with the provided recombinant standards.

Detection of Fe^{2+}, Glutathione (GSH), and Reactive Oxygen Species (ROS) Levels

Following standardized protocols provided by the manufacturers, intracellular Fe^{2+}, GSH, and ROS levels in transfected and/or KA-treated HT22 cells were quantified using commercial assay kits: Ferrous Iron Colorimetric Assay Kit (Catalog #E-BC-K881-M, Elabscience, Wuhan, China), GSH Assay Kit (Catalog #ab239709, Abcam), and 2',7'-dichlorodihydrofluorescein diacetate (DCFH-DA) ROS Detection Kit (Catalog #S0036S, Beyotime). For quantification of Fe^{2+} and GSH levels, absorbance (OD = 593 nm for Fe^{2+} and 412 nm for GSH) was measured using the Infinite® M200 PRO reader. Fe^{2+} concentration was calculated based on the standard curve prepared from the provided ferrous iron standard. GSH levels were determined by measuring the absorbance of the reaction product at 412 nm and calculating concentrations from a GSH standard curve. ROS levels were detected using fluorescence imaging on a Leica SP8 microscope (Model #TCS SP8, Leica, Wetzlar, Germany) and flow cytometric analysis with LSRII system. For flow cytometry analysis, the mean fluorescence intensity (MFI) of ROS was measured and expressed as a fold change relative to the control group.

Prediction of the E3 Ubiquitin Ligases for KEAP1 Ubiquitination

The Ubibrowser2.0 web server (http://ubibrowser.bio-it.cn/ubibrowser_v3/) was employed to predict candidate E3 ubiquitin ligases potentially involved in KEAP1 ubiquitination, with the Mus musculus genome setting.

Immunoprecipitation (IP) and Co-immunoprecipitation (Co-IP) Experiments

HT22 neurons transfected with or without OE-NC, OE-PRKN, si-NC, or si-HDAC6 were examined for Co-IP and IP assays using a commercial IP Kit (Catalog #P1836S, Beyotime) with antibodies against PRKN (Catalog #14060-1-AP, Proteintech, Wuhan, China), KEAP1 (Catalog #10503-2-AP, Proteintech), HDAC6 (Catalog #ab264565, Abcam), and IgG (Catalog #98136-1-RR, Proteintech). Briefly, whole-cell lysates were prepared and incubated with Protein A magnetic beads that had been pre-coated with the relevant antibody. After immunocomplex isolation, bound proteins were obtained by boiling in SDS loading buffer for 5 min and subsequently analyzed by immunoblotting to assess the enriched protein levels of KEAP1, PRKN, HDAC6, ubiquitinated KEAP1, and acetylated-PRKN.

Analysis of KEAP1 Protein Stabilization

To assess the impact of PRKN on KEAP1 protein stability, HT22 neurons subjected to transfection with OE-NC or OE-PRKN were cultured in complete medium supplemented with 20 ng/mL cycloheximide (CHX, Catalog #S7418, Selleckchem) [25] for specified durations (0, 5, 10, and 20 h). After that, the levels of remaining KEAP1 protein were evaluated using immunoblot analysis.

Prediction of Potential PRKN-interacting Proteins

Proteins that interacted with PRKN were predicted using the STRING algorithm (Version 12.0) (https://cn.string-db.org/).

Statistical Analysis

All data were expressed as mean ± standard deviation (SD) from a minimum of three independent biological replicates. Statistical analyses were performed using GraphPad Prism version 8.0.2 (GraphPad Software, San Diego, CA, USA). Comparisons were made using two-tailed Student's *t*-test or one-way analysis of variance (ANOVA) followed by Tukey's post hoc test, depending on experimental design. A *p*-value threshold of <0.05 was considered statistically significant, with asterisks denoting the degree of significance in the figures.

Results

KEAP1 Knockdown Reverses KA-induced Neuroinflammation and Ferroptosis in HT22 Cells

To further elucidate the function of KEAP1 in neuronal cytotoxicity, this study first generated a KA-induced HT22 neurotoxicity model. Notably, the protein levels of KEAP1 in the model were significantly upregulated compared with the corresponding control ($p = 0.0008$, Fig. 1A). Functionally, KA-stimulated HT22 cells exhibited significantly impaired cell viability ($p = 0.0005$, Fig. 1B) and enhanced apoptosis ($p < 0.001$, Fig. 1C) when compared with sham controls. Moreover, KA exposure increased the production of pro-inflammatory cytokines IL-6 ($p = 0.0001$), TNF-α ($p < 0.001$), and IL-1β ($p = 0.0002$), while reducing the expression of anti-inflammatory cytokine IL-10 ($p = 0.003$) in HT22 cells (Fig. 1D,E and **Supplementary Fig. 1A,B**). KEAP1 depletion was then performed with a specific siRNA (si-KEAP1) in the cellular model to observe the consequences. Notably, silencing of KEAP1 via si-KEAP1 transfection, verified by immunoblot analysis ($p = 0.0017$, Fig. 1A), strongly restored cell viability ($p = 0.0055$, Fig. 1B), diminished cell apoptosis ($p = 0.0016$,

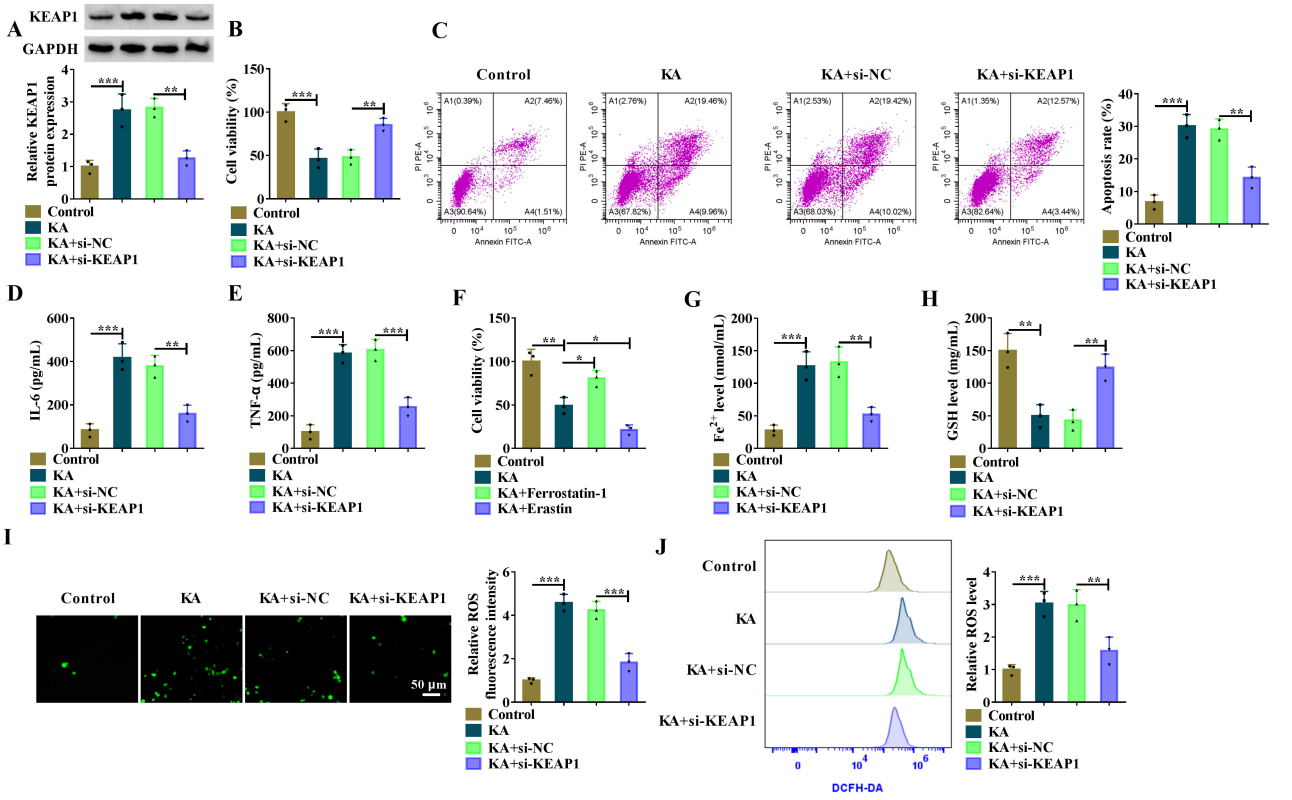

Fig. 1. KEAP1 mediates inflammation and ferroptosis in KA-induced HT22 neuronal cells. (A–E) HT22 hippocampal neuronal cells were stimulated with KA or vehicle sham or transfected with si-KEAP1 or si-NC prior to KA stimulation. (A) Representative immunoblot of treated HT22 cells and quantification of KEAP1 protein expression. (B) Viability of treated HT22 cells by MTT assay. (C) Apoptosis of treated HT22 cells by flow cytometry. (D,E) Levels of IL-6 and TNF-α cytokines in the medium of treated HT22 cells using ELISA. (F) MTT assay for viability of HT22 cells treated with sham, KA, KA+Ferrostatin-1, or KA+Erastin. (G,H) Levels of Fe^{2+} and GSH in HT22 cells treated as A–E. (I,J) Representative fluorescence images and flow cytometry analysis of HT22 cells treated as A–E and quantification of relative ROS content. *$p < 0.05$, **$p < 0.01$, ***$p < 0.001$. KA, kainic acid; KEAP1, Kelch-like ECH-associated protein 1; MTT, 3-(4,5-dimethylthiazol-2-yl)-2,5-diphenyltetrazolium bromide; ELISA, enzyme-linked immunosorbent assay; GSH, glutathione; ROS, reactive oxygen species.

Fig. 1C), and reversed the KA-induced alterations of IL-6 ($p = 0.0021$), TNF-α ($p = 0.0003$), IL-1β ($p = 0.0015$), and IL-10 ($p = 0.0124$) secretion levels (Fig. 1D,E and **Supplementary Fig. 1A,B**).

Ferroptosis has emerged as a key contributor to epilepsy pathogenesis, promoting to neuronal loss and disease progression [26]. To evaluate whether ferroptosis is responsible for KA-induced viability loss, KA-induced HT22 cells were exposed to either the ferroptosis inhibitor Ferrostatin-1 or the ferroptosis inducer Erastin. As expected, treatment of Ferrostatin-1 rescued KA-caused viability loss ($p = 0.0198$), while Erastin exposure exacerbated KA-induced viability impairment ($p = 0.0389$) in HT22 cells (Fig. 1F), demonstrating the contribution of ferroptosis to KA-mediated cytotoxicity. Intriguingly, KA-induced HT22 cells increased Fe^{2+} levels ($p = 0.0006$, Fig. 1G), reduced GSH content ($p = 0.0015$, Fig. 1H), and elevated ROS amount ($p < 0.001$, Fig. 1I,J) compared to control cells, indicating that KA-induced HT22 cells enhance ferroptosis. However, KEAP1 knockdown attenuated ferroptosis induced by KA, as presented by decreased Fe^{2+} ($p = 0.0022$) and ROS ($p < 0.01$) levels and elevated GSH content ($p = 0.0057$) following KEAP1 knockdown in KA-induced HT22 cells (Fig. 1G–J). Taken together, our data suggest that KEAP1 is upregulated in the KA-induced HT22 cells and is responsible for enhanced inflammation and ferroptosis.

PRKN Mediates KEAP1 Ubiquitination and Degradation, Thereby Alleviating Inflammation and Ferroptosis in KA-Induced HT22 Cells

Ubiquitination of KEAP1 can lead to the activation of NRF2, thereby playing critical roles in human disorders [27,28]. Among candidate E3 ubiquitin ligases predicted via Ubibrowser screening, PRKN was prioritized for experimental validation (Fig. 2A). This selection was based on its well-established neuroprotective functions, including maintaining mitochondrial homeostasis and mitigating ox-

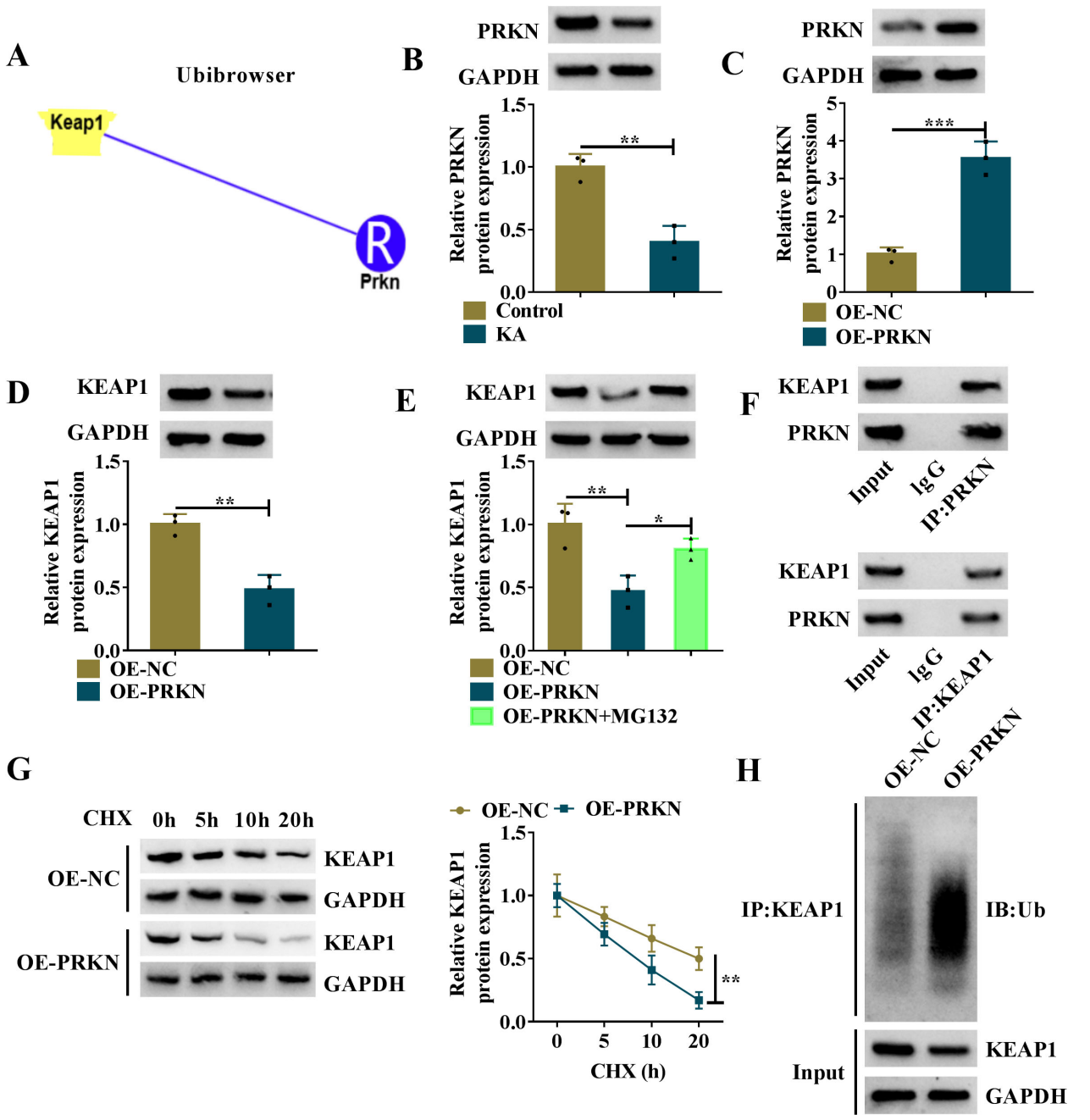

Fig. 2. PRKN mediates KEAP1 ubiquitination and degradation. (A) Schematic model of the relationship between PRKN and KEAP1 through Ubibrowser screening. (B) Representative immunoblot of HT22 cells treated with vehicle or KA and quantification of PRKN protein expression. (C,D) Representative immunoblot of HT22 cells transfected with OE-NC or OE-PRKN and quantification of PRKN (C) and KEAP1 (D) protein expression. (E) Immunoblot of KEAP1 protein in OE-NC- or OE-PRKN-transfected HT22 cells with or without MG132 treatment. (F) Co-IP experiments using an anti-PRKN or anti-KEAP1 antibody with lysates of HT22 cells, and the subsequent immunoblot analysis of proteins bound to immunoprecipitates. (G) Representative immunoblot of HT22 cells transfected with OE-NC or OE-PRKN under CHX treatment and quantification of the remaining KEAP1 protein. (H) IP assays using an anti-KEAP1 antibody with lysates of OE-NC- or OE-PRKN-transfected HT22 cells, and the subsequent immunoblot analysis of ubiquitinated KEAP1. $*p < 0.05$, $**p < 0.01$, $***p < 0.001$. CHX, cycloheximide; PRKN, parkin RBR E3 ubiquitin protein ligase; Co-IP, co-immunoprecipitation; IP, immunoprecipitation.

idative stress in neurological disorders [29,30], alongside a recent report that PRKN promotes ACSL1 ubiquitination and activates the anti-ferroptotic NRF2/SLC7A11/GPX4 pathway [16]. These previous findings suggest PRKN as

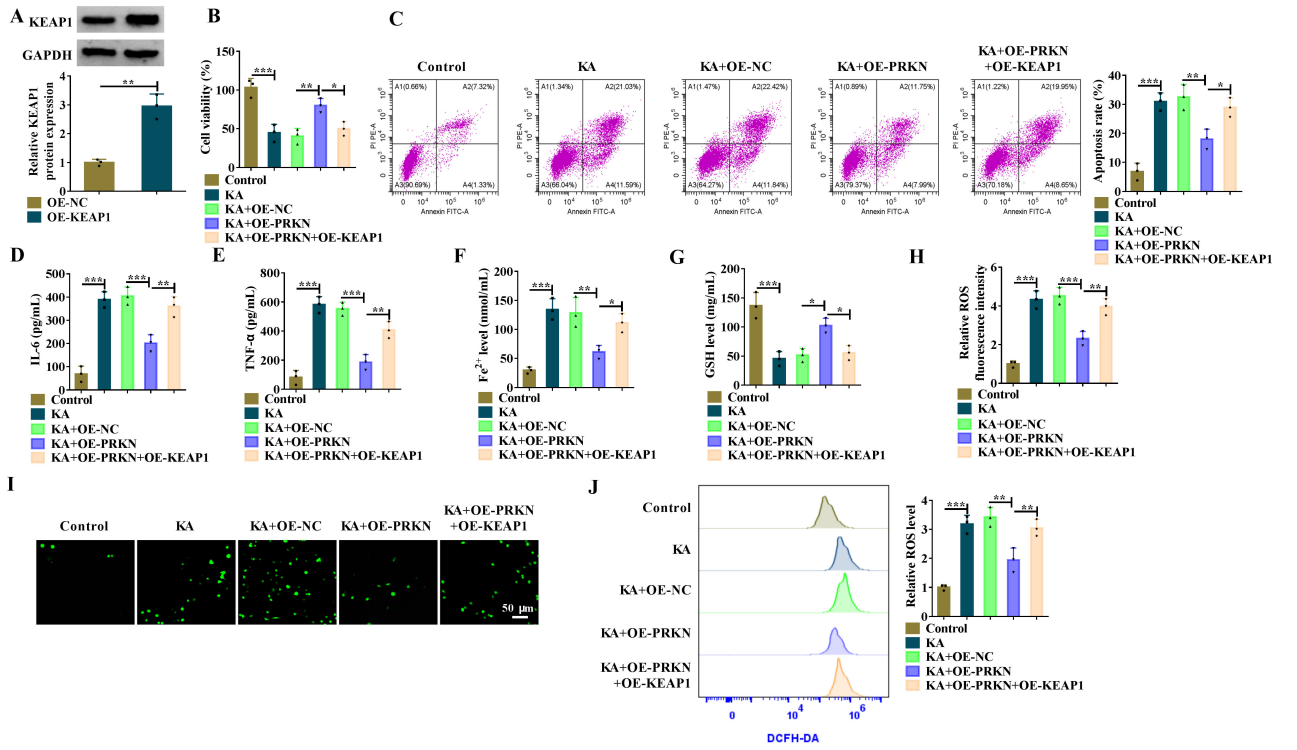

Fig. 3. The PRKN-KEAP1 axis mediates KA-induced neuroinflammation and ferroptosis in HT22 neuronal cells. (A) Representative immunoblot of HT22 cells transfected with OE-NC or OE-KEAP1 and quantification of KEAP1 protein expression. (B–J) HT22 hippocampal neuronal cells were stimulated with KA or vehicle or transfected with OE-NC, OE-PRKN, or OE-PRKN+OE-KEAP1 prior to KA stimulation. (B) Cell viability assessed by MTT assay. (C) Apoptosis rate measured by flow cytometry. (D,E) Secreted IL-6 and TNF-α levels measured by ELISA. (F,G) Intracellular Fe^{2+} and GSH contents using the assay kits. (H–J) ROS production analyzed by fluorescence microscopy (H,I) and flow cytometry (J). *$p < 0.05$, **$p < 0.01$, ***$p < 0.001$.

a potential regulator of the KEAP1/NRF2 axis. Contrary to KEAP1 expression, KA-induced HT22 cells exhibited lower protein levels of PRKN than sham controls (p = 0.0034, Fig. 2B). To clarify the precise role of PRKN in regulating KEAP1, this study first examined its effect on KEAP1 expression. HT22 cells were transfected with a PRKN expression plasmid (OE-PRKN) to increase PRKN expression. Upregulation of PRKN upon OE-PRKN introduction, confirmed by immunoblot assay (p = 0.0008, Fig. 2C), resulted in decreased expression of KEAP1 protein (p = 0.0032, Fig. 2D). Notably, treatment with the proteasome inhibitor MG132 abolished the PRKN-mediated reduction in KEAP1 protein levels in HT22 cells (p = 0.0446, Fig. 2E). Our study then evaluated the interaction between PRKN and KEAP1. After Co-IP experiments using an anti-PRKN antibody, immunoblot analysis revealed that KEAP1 was observed in PRKN immunoprecipitates (Fig. 2F). Reciprocally, PRKN was observed in KEAP1 immunoprecipitates (Fig. 2F). This study also tested whether PRKN modulates KEAP1 protein stability. Under CHX conditions for translational suppression, increased PRKN expression markedly reduced KEAP1 stabilization (p = 0.0054, Fig. 2G). Next, this study assessed whether PRKN is indeed able to catalyze ubiquitination and degradation of KEAP1 protein in HT22 cells. As illustrated in Fig. 2H, the levels of ubiquitinated KEAP1 were increased after overexpression of PRKN. Together, these findings establish the fact that KEAP1 is a *bona fide* substrate of PRKN.

To understand the functional consequence of this interaction in KA-induced neuronal cytotoxicity, this study transfected OE-PRKN alone or with a KEAP1 expression vector (OE-KEAP1) into HT22 cells and primary hippocampal neurons before KA exposure. Upregulation of PRKN mediated by OE-PRKN in primary hippocampal neurons was confirmed by immunoblot assay (p = 0.0008, **Supplementary Fig. 2A**). Immunoblot analysis confirmed the upregulation efficiency of OE-KEAP1 in KEAP1 expression ($p < 0.01$, Fig. 3A and **Supplementary Fig. 2B**). In the KA-induced HT22 cells and primary hippocampal neurons, increased PRKN expression conferred neuroprotection by enhancing cell viability ($p < 0.01$, Fig. 3B and **Supplementary Fig. 2C**), suppressing cell apoptosis ($p <$ 0.01, Fig. 3C and **Supplementary Fig. 2D,E**), reducing IL-6 and TNF-α levels ($p < 0.01$, Fig. 3D,E and **Supplementary Fig. 2F**), decreasing Fe^{2+} content (p = 0.0048, Fig. 3F), increasing GSH amount (p = 0.013, Fig. 3G), and

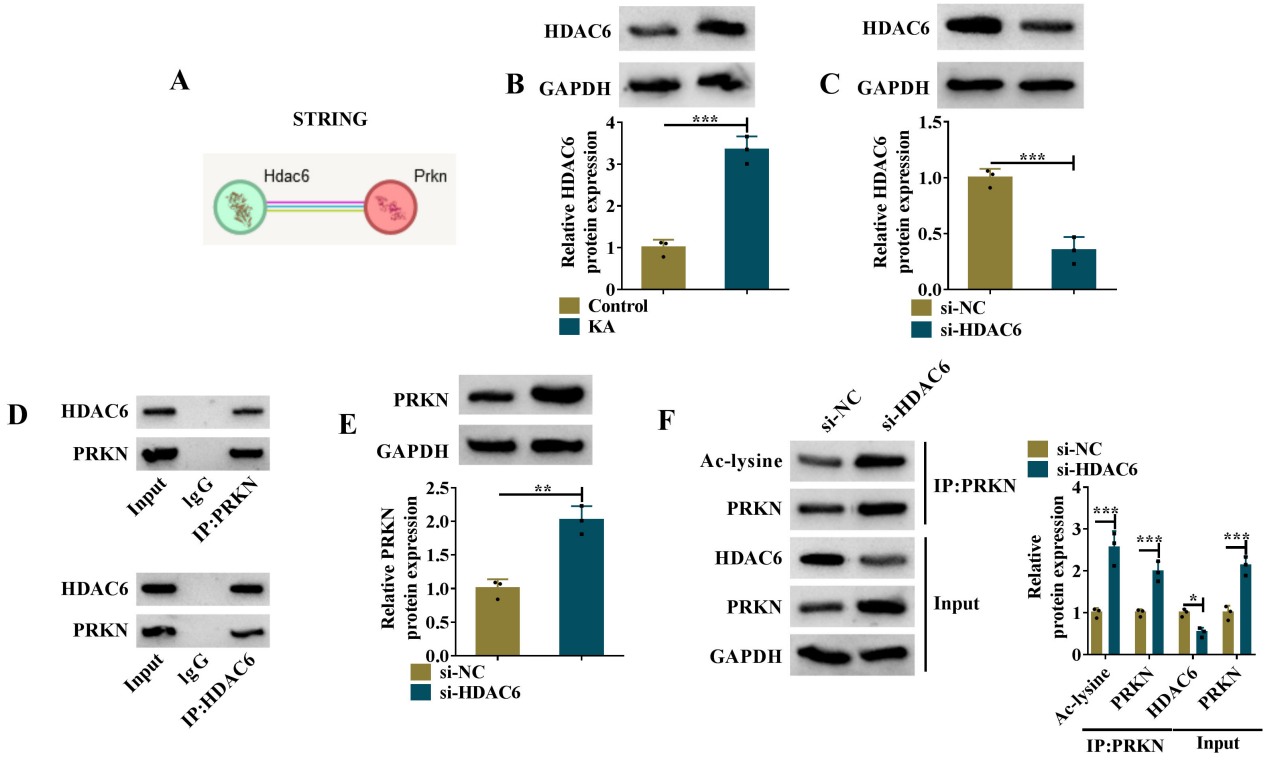

Fig. 4. Deacetylation of PRKN is mediated by HDAC6. (A) Schematic of the interaction between HDAC6 and PRKN using the STRING algorithm. (B) Representative immunoblot of HT22 cells treated with vehicle or KA and quantification of HDAC6 protein expression. (C) Representative immunoblot of HT22 cells transfected with si-NC or si-HDAC6 and quantification of HDAC6 protein expression. (D) Co-IP assays were performed using HT22 cell lysates with either an anti-PRKN or anti-HDAC6 antibody, followed by immunoblotting analysis of the precipitated protein complexes. (E) Representative immunoblot of si-NC- or si-HDAC6-transfected HT22 cells and quantification of the PRKN protein. (F) IP assays using an anti-PRKN antibody with lysates of si-NC- or si-HDAC6-transfected HT22 cells, and the subsequent immunoblot analysis of acetylated PRKN. *$p < 0.05$, **$p < 0.01$, ***$p < 0.001$. HDAC6, histone deacetylase 6.

downregulating ROS production ($p < 0.01$, Fig. 3H–J and **Supplementary Fig. 2G**). Notably, these protective effects were significantly counteracted by KEAP1 reconstitution ($p < 0.05$, Fig. 3B–J and **Supplementary Fig. 2C–G**). Collectively, these results demonstrate the involvement of the PRKN-KEAP1 axis in KA-induced neuroinflammation and ferroptosis in neuronal cells.

HDAC6 Mediates Deacetylation of PRKN

Using the STRING algorithm, HDAC6, a crucial deacetylase associated with epilepsy pathogenesis [18], was predicted to physically interact with PRKN (Fig. 4A). Given that HDAC6 inhibition synergistically suppresses ferroptosis, a process implicated in neurodegeneration [20], and considering the established role of PRKN in regulating anti-ferroptotic pathways, we hypothesized that the interaction between HDAC6 and PRKN may play a functionally significant role in our model. Supporting this notion, HDAC6 protein levels were significantly elevated in KA-induced HT22 cells ($p = 0.0004$), contrasting with the reduction in PRKN (Fig. 4B). HT22 cells were transfected with a HDAC6-specific siRNA (si-HDAC6), which effectively knocked down HDAC6 expression as confirmed by immunoblotting ($p = 0.0009$, Fig. 4C). To investigate HDAC6's regulatory effects on PRKN, this study first verified their physical interaction. Co-IP assays using an anti-PRKN antibody, followed by immunoblotting, demonstrated HDAC6 presence in PRKN immunoprecipitates (Fig. 4D). Reciprocally, Co-IP assays using an anti-HDAC6 antibody identified PRKN in the precipitated complexes (Fig. 4D). Subsequent experiments examined the functional implications of this interaction. Notably, siRNA-mediated HDAC6 downregulation resulted in a significant elevation of PRKN protein levels ($p = 0.0022$, Fig. 4E). Our study further investigated whether HDAC6 mediates PRKN deacetylation in HT22 neurons. Immunoblot analysis after Co-IP assays showed enhanced PRKN acetylation following HDAC6 depletion ($p < 0.001$, Fig. 4F). All these data suggest that deacetylation of PRKN is induced by HDAC6.

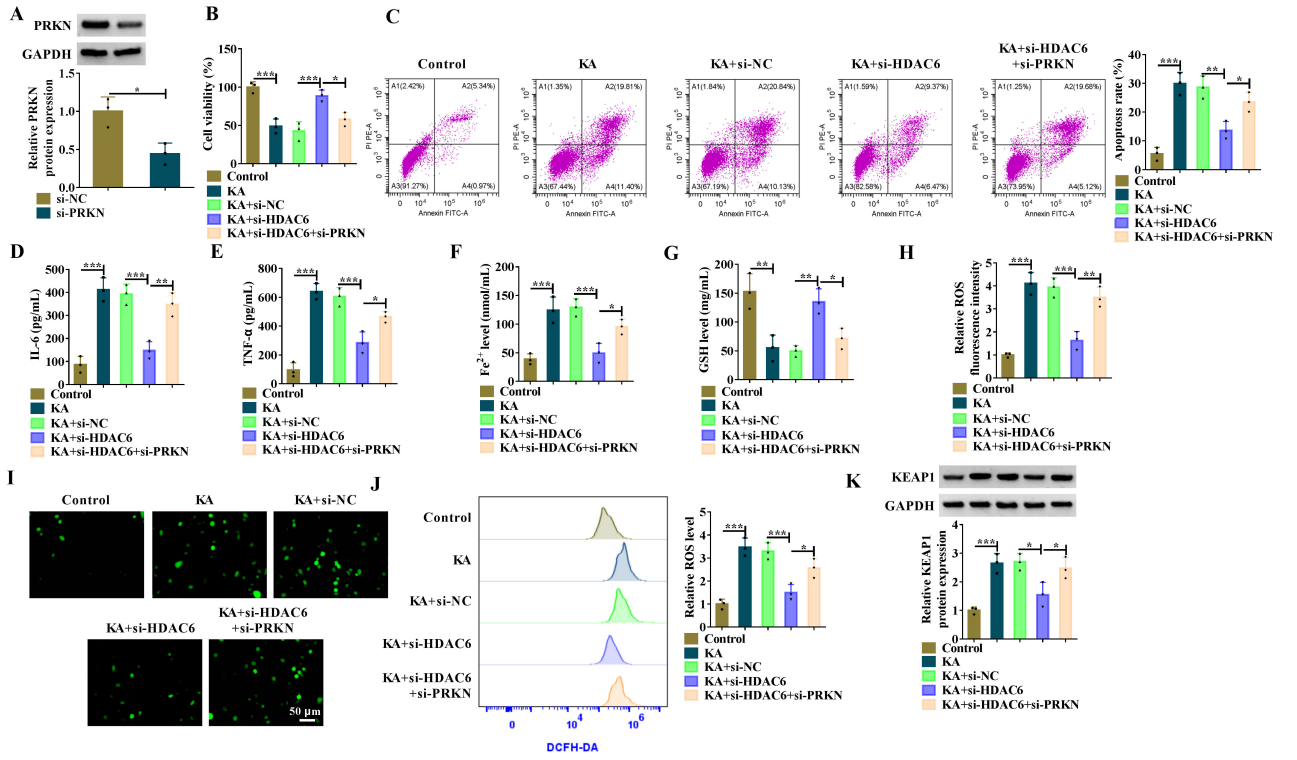

Fig. 5. The HDAC6-PRKN axis regulates KA-induced neuroinflammatory responses and ferroptotic pathways in HT22 neuronal cells. (A) Representative immunoblot of HT22 cells transfected with si-NC or si-PRKN and quantification of PRKN protein expression. (B–K) HT22 hippocampal neurons were stimulated with KA or vehicle or transfected with si-NC, si-HDAC6, or si-HDAC6+si-PRKN prior to KA stimulation. (B) Cell viability assessed by MTT assay. (C) Flow cytometry for apoptosis rate of treated HT22 cells. (D,E) IL-6 and TNF-α secretion levels measured by ELISA. (F,G) Fe^{2+} and GSH levels in treated HT22 cells using the assay kits. (H–J) ROS production analyzed by fluorescence microscopy (H,I) and flow cytometry (J). (K) Immunoblot assay of KEAP1 protein in treated HT22 cells. *$p < 0.05$, **$p < 0.01$, ***$p < 0.001$.

PRKN Knockdown Counteracts si-HDAC6-Mediated Anti-Inflammatory and Ferroptosis-Inhibitory Effects in KA-Induced HT22 Cells

To elucidate the functional relationship between HDAC6 and PRKN in KA-induced HT22 neuronal injury, this study transfected si-HDAC6 alone or together with a siRNA targeting PRKN (si-PRKN) into HT22 cells prior to KA induction. Immunoblot assay showed efficient PRKN silencing in the si-PRKN transfected cells ($p = 0.0150$, Fig. 5A). HDAC6 knockdown provided significant neuroprotection in the KA-induced HT22 cells. First, it markedly improved neuronal viability ($p = 0.0008$, Fig. 5B) while reducing apoptotic cell death ($p = 0.0019$, Fig. 5C). Second, it substantially decreased the production of pro-inflammatory cytokines IL-6 ($p = 0.0004$) and TNF-α ($p = 0.0004$, Fig. 5D,E). Third, HDAC6 knockdown restored oxidative balance by decreasing Fe^{2+} content ($p = 0.0009$, Fig. 5F), increasing GSH amount ($p = 0.0054$, Fig. 5G), and effectively diminishing ROS production ($p < 0.001$, Fig. 5H–J). Importantly, when PRKN expression was simultaneously reduced, these protective effects were significantly abolished ($p < 0.05$, Fig. 5B–J). In addition, in the cellular model, HDAC6 downregulation resulted in decreased protein levels of KEAP1 ($p = 0.0108$), which was reversed by PRKN reduction ($p = 0.0224$, Fig. 5K), indicating the modulation of HDAC6 in KEAP1 expression via PRKN. These findings demonstrate that the HDAC6-PRKN interaction plays a key role in regulating KA-induced neuroinflammatory responses and ferroptotic pathways in HT22 neuronal cells.

PRKN Regulates the NRF2/SLC7A11/GPX4 Pathway Through KEAP1

The NRF2/SLC7A11/GPX4 pathway plays a neuroprotective role in epilepsy by suppressing ferroptosis, reducing oxidative stress, and preserving neuronal viability [31]. Suppression of KEAP1 leads to the activation of NRF2, thereby mitigating oxidative stress and ferroptosis [32,33]. Since PRKN mediates KEAP1 ubiquitination and degradation, this study sought to investigate the regulation of PRKN in this pathway. In the KA-induced HT22 neuronal cells, the protein levels of NRF2 ($p = 0.0012$), SLC7A11 ($p = 0.0033$), and GPX4 ($p = 0.0002$) were significantly downregulated compared with control cells

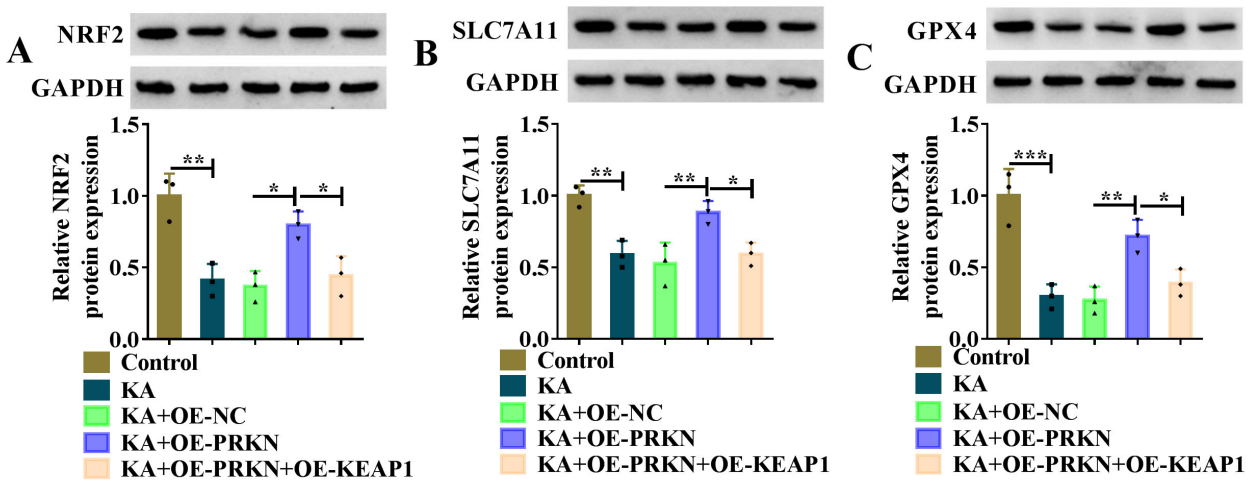

Fig. 6. PRKN regulates the NRF2/SLC7A11/GPX4 pathway through KEAP1. (A–C) HT22 hippocampal neurons were stimulated with KA or vehicle or transfected with OE-NC, OE-PRKN, or OE-PRKN+OE-KEAP1 prior to KA stimulation. Representative immunoblot of treated HT22 cells and quantification of NRF2 (A), SLC7A11 (B), and GPX4 (C) proteins. *$p < 0.05$, **$p < 0.01$, ***$p < 0.001$. NRF2, nuclear factor erythroid 2-related factor 2; SLC7A11, solute carrier family 7 member 11; GPX4, glutathione peroxidase 4.

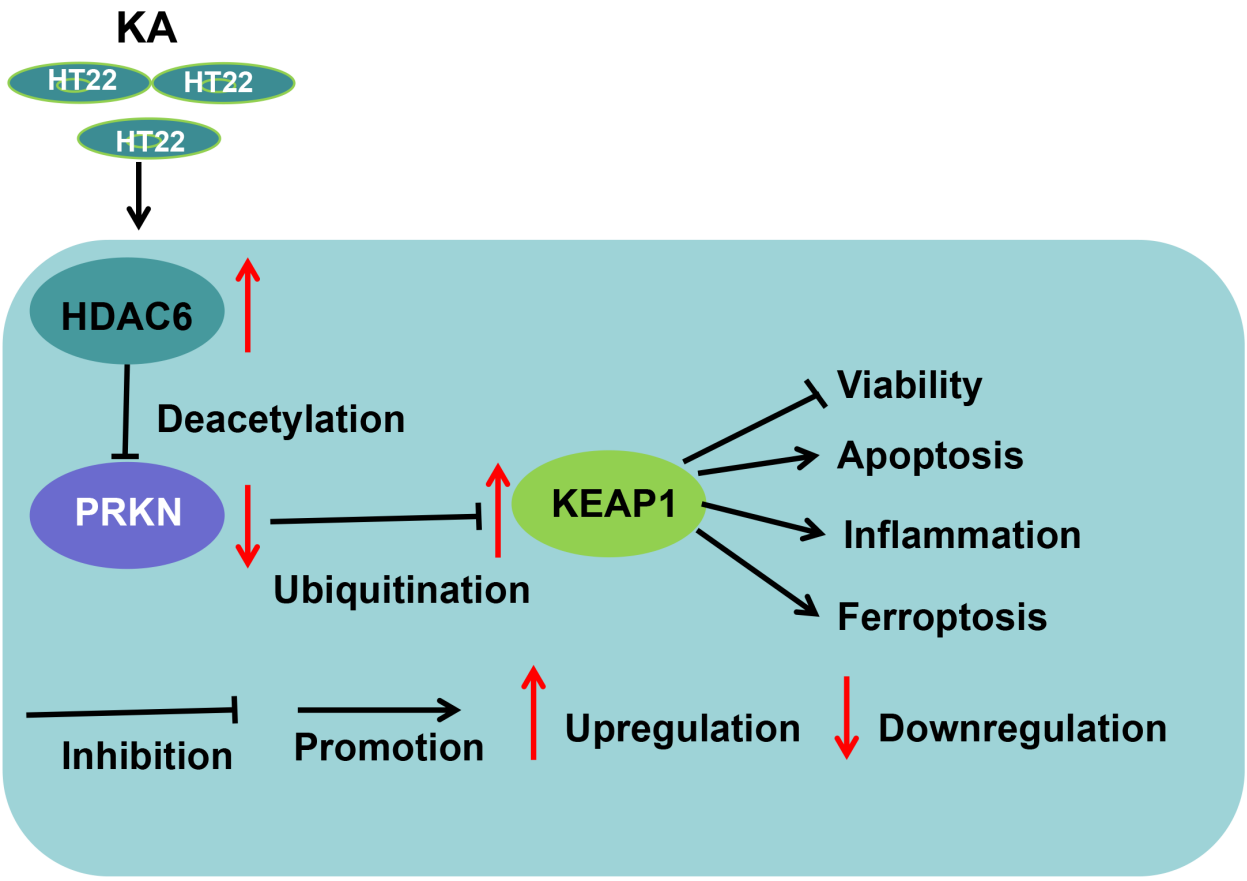

Fig. 7. Schematic model of the HDAC6-PRKN-KEAP1 cascade in modulating ferroptosis and neuroinflammation in KA-induced HT22 neuronal cells. In this model, HDAC6 induces PRKN deacetylation, and then PRKN mediates KEAP1 ubiquitination and degradation, thereby modulating cell ferroptosis, apoptosis, viability, and neuroinflammation.

(Fig. 6A–C). When PRKN expression was increased, the levels of these proteins were strongly upregulated in KA-treated HT22 cells; however, increased KEAP1 expression counteracted these effects (Fig. 6A–C). Furthermore, the NRF2 inhibitor ML385 could reverse KEAP1 knockdown-mediated viability promotion ($p = 0.0355$, **Supplementary Fig. 3A**), apoptosis repression ($p = 0.0293$, **Supplementary Fig. 3B**), IL-6 ($p = 0.0162$) and TNF-α ($p = 0.0025$) reduction (**Supplementary Fig. 3C,D**), and ferroptosis suppression ($p < 0.05$, **Supplementary Fig. 3E–G**) in KA-treated HT22 cells. These data together indicate the regulation of the PRKN-KEAP1 axis in KA-induced neurotoxicity in HT22 cells through the NRF2/SLC7A11/GPX4 pathway.

Discussion

Ferroptosis significantly contributes to neuronal death and cognitive deficits in experimental epilepsy, and its inhibition—through agents such as coenzyme Q10 (CoQ10), ferrostatin-1, or a ketogenic diet—effectively provides neuroprotection [34–36]. KEAP1 can promote NRF2 ubiquitination and degradation under physiological conditions, but oxidative stress disrupts this interaction, enabling NRF2 to activate cytoprotective genes, thereby protecting cells against oxidative damage [8]. Emerging studies also unveil the crucial regulation of the KEAP1/NRF2 interaction in ferroptosis during various pathological conditions, such as acute lung injury and atherosclerosis [32,37]. In epilepsy, KEAP1 overexpression exacerbates neuronal damage and seizure recurrence by impairing antioxidant defenses and amplifying oxidative stress and neuroinflammation [13,38]. Moreover, inhibition of KEAP1 stabilizes NRF2, enhancing cellular defenses against oxidative stress and iron overload, ultimately mitigating ferroptosis in epileptic neurons [39]. Consistent with these reports, our findings demonstrate that KEAP1 depletion attenuates KA-induced ferroptosis and inflammation in HT22 neuronal cells. These findings suggest that KEAP1 hyperactivation contributes to hippocampal neuronal injury by promoting neuroinflammation and ferroptosis. This aligns with previous studies linking dysfunction of KEAP1/NRF2 axis to neurodegenerative disorders, where KEAP1 inhibition confers neuroprotection through NRF2-mediated antioxidant and anti-inflammatory pathways [40,41].

PRKN, a pivotal regulator of mitophagy and cellular stress responses, has emerged as a critical player in diminishing ferroptosis. Specifically, PRKN-mediated mitophagy maintains mitochondrial homeostasis by eliminating damaged mitochondria, thereby mitigating lipid peroxidation and iron overload, which are key drivers of ferroptosis [42]. Dysregulation of PRKN is implicated in neurodegenerative disorders, such as Parkinson's and Alzheimer's diseases, where unbalanced protein ubiquitination and impaired mitophagy exacerbate neuronal vulnerability to oxidative stress [43,44]. In epilepsy, recent evidence suggests altered PRKN expression correlates with neuronal hyperexcitability and oxidative stress, though its mechanistic contributions remain underexplored [45]. Our study revealed a mechanistic role for PRKN in mediating KEAP1 ubiquitination and degradation, which alleviates ferroptosis and inflammation in the KA-induced HT22 neuronal cells.

HDAC6, a unique cytosolic deacetylase, regulates ferroptosis by modulating lipid peroxidation enzymes and iron metabolism proteins, linking epigenetic modifications to redox imbalance in neurological disorders [20]. HDAC6 overexpression exacerbates neuroinflammation and neurodegeneration in Alzheimer's and Parkinson's diseases, and inhibition of HDAC6 exerts neuroprotective effects in these disorders [46,47]. In epilepsy, HDAC6 upregulation correlates with aberrant synaptic plasticity and neuronal hyperexcitability, while its inhibition attenuates seizure severity in preclinical models [18,19]. Our results reveal that HDAC6 mediates the deacetylation of PRKN, thereby promoting KA-induced neuroinflammation and ferroptosis in HT22 cells. More importantly, our results demonstrate HDAC6 regulates KEAP1 expression via PRKN. These findings identify the HDAC6-PRKN-KEAP1 axis as a potential regulator of KA-induced neurotoxicity.

The NRF2/SLC7A11/GPX4 axis, a central regulatory cascade in cellular antioxidant defense, plays a dual role in modulating ferroptosis and neurological disorders [48,49]. Mechanistically, NRF2 activation transcriptionally upregulates SLC7A11 to enhance cystine uptake and glutathione synthesis, while GPX4 utilizes glutathione to neutralize lipid peroxides, thereby suppressing ferroptosis [50]. In epilepsy, emerging evidence suggests that impaired NRF2/SLC7A11/GPX4 signaling contributes to seizure-induced neuronal death [31]. Moreover, KEAP1 suppression results in NRF2 stabilization and subsequent nuclear translocation, activating antioxidant responses that attenuate oxidative stress and inhibit ferroptosis [32,33]. Our study identifies PRKN as a critical upstream modulator of the NRF2/SLC7A11/GPX4 axis via KEAP1. PRKN-mediated KEAP1 ubiquitination and degradation stabilize NRF2, amplifying SLC7A11 and GPX4 expression to counteract ferroptosis and neuroinflammation in the KA-induced HT22 neuronal cells. Notably, a key limitation of this study lies in the absence of pathway-specific pharmacological interventions (e.g., NRF2 inhibitors or GPX4 activators). Without these controls, it remains challenging to determine whether the observed effects of the HDAC6-PRKN-KEAP1 axis are directly mediated via this pathway. Future studies could clarify whether the observed effects are pathway-dependent.

In addition, several limitations and future directions should be considered. First, while the present study offers valuable mechanistic insights, its exclusive reliance on the *in vitro* HT22 neuronal model inherently limits the ability to fully recapitulate the complex, multi-cellular pathophysiology of epilepsy *in vivo*. Key aspects such as network-

level synchronization, glia-neuron interactions, vascular contributions, and systemic inflammatory responses are not represented in this system. Further validation in established animal models of epilepsy would significantly strengthen the translational impact of these findings. For example, employing a KA-induced murine model of status epilepticus would allow us to: (1) confirm the role of KEAP1 in modulating ferroptosis and neuroinflammation within a more complex, integrated physiological environment; (2) assess the effect of KEAP1 manipulation on electrographic seizure activity and behavioral outcomes; and (3) investigate cell-type-specific contributions (e.g., astrocytes, microglia) to the observed mechanisms. Second, although our study demonstrated that PRKN mediates KEAP1 ubiquitination and HDAC6 mediates PRKN deacetylation, the precise modification sites—the ubiquitination sites on KEAP1 and the deacetylation sites on PRKN—remain unmapped. Identification of these specific residues is crucial for mechanistic understanding of the regulatory interplay between these proteins. Further studies employing mass spectrometry-based proteomics or site-directed mutagenesis will be essential to precisely delineate these modification sites and validate their functional roles within the KEAP1-PRKN-HDAC6 signaling axis. Third, the translational relevance of this signaling axis requires further validation. The current study lacks functional experiments using specific HDAC6 inhibitors or PRKN activators within *in vivo* seizure models, which limits assessment of its therapeutic potential for seizure control or neuroprotection. Future studies employing both genetic and pharmacological approaches, such as Tubastatin A for HDAC6 inhibition or PRKN overexpression, in established animal models of epilepsy will be critical to confirm the pathway's role in seizure pathophysiology and to assess its suitability as an anti-epileptogenic target. Additionally, the present study primarily employed the HT22 neuronal cell line, which lacks functional ionotropic glutamate receptors, indicating that the observed KA-induced toxicity likely operates through mechanisms distinct from classical receptor-mediated excitotoxicity. While this model limitation necessitates caution in extrapolating to all excitotoxic contexts, complementary validation in primary hippocampal neurons confirms the broader relevance of the identified PRKN-KEAP1 cascade in modulating neuronal ferroptosis and inflammation.

Conclusion

Overall, our findings highlight the crucial role of the novel HDAC6-PRKN-KEAP1 cascade in modulating ferroptosis and neuroinflammation in KA-induced HT22 neuronal cells (Fig. 7). These findings advance the mechanistic understanding of neurotoxicity and identify this cascade as a potential therapeutic target for protecting neurons from damage.

Availability of Data and Materials

The data that support the findings of this study are available from the corresponding author upon reasonable request.

Author Contributions

TW and YL designed the research study. JH and YZ performed the research. YL and YZ analyzed the data. JH, TW and YL drafted the article. All authors contributed to important editorial changes in the manuscript. All authors read and approved the final manuscript. All authors have participated sufficiently in the work and agreed to be accountable for all aspects of the work.

Ethics Approval and Consent to Participate

Not applicable.

Acknowledgment

Not applicable.

Funding

This research received no external funding.

Conflict of Interest

The authors declare no conflict of interest.

Supplementary Material

Supplementary material associated with this article can be found, in the online version, at https://doi.org/10.24976/Discov.Med.202638206.73.

References

[1] Falco-Walter J. Epilepsy-Definition, Classification, Pathophysiology, and Epidemiology. Seminars in Neurology. 2020; 40: 617–623. https://doi.org/10.1055/s-0040-1718719.

[2] Miller JW. Inflammation as a Target for Epilepsy Therapy: The Case of Natalizumab. Neurology. 2021; 97: 845–846. https://doi.org/10.1212/WNL.0000000000012768.

[3] Kamieniak M, Kośmider K, Miziak B, Czuczwar SJ. The Oxidative Stress in Epilepsy-Focus on Melatonin. International Journal of Molecular Sciences. 2024; 25: 12943. https://doi.org/10.3390/ijms252312943.

[4] Thom M. Review: Hippocampal sclerosis in epilepsy: a neuropathology review. Neuropathology and Applied Neurobiology. 2014; 40: 520–543. https://doi.org/10.1111/nan.12150.

[5] Wang ZL, Yuan L, Li W, Li JY. Ferroptosis in Parkinson's disease: glia-neuron crosstalk. Trends in Molecular Medicine. 2022; 28: 258–269. https://doi.org/10.1016/j.molmed.2022.02.003.

[6] Wang T, Tomas D, Perera ND, Cuic B, Luikinga S, Viden A, *et al*. Ferroptosis mediates selective motor neuron death in amy-

otrophic lateral sclerosis. Cell Death and Differentiation. 2022; 29: 1187–1198. https://doi.org/10.1038/s41418-021-00910-z.

[7] Chen S, Zhao L, Jin X, Liu Q, Xiao Y, Xu H. Astaxanthin Inhibits Ferroptosis of Hippocampal Neurons in Kainic Acid-Induced Epileptic Mice by Activating the Nrf2/GPX4 Signaling Pathway. CNS Neuroscience & Therapeutics. 2025; 31: e70238. https://doi.org/10.1111/cns.70238.

[8] Yamamoto M, Kensler TW, Motohashi H. The KEAP1-NRF2 System: a Thiol-Based Sensor-Effector Apparatus for Maintaining Redox Homeostasis. Physiological Reviews. 2018; 98: 1169–1203. https://doi.org/10.1152/physrev.00023.2017.

[9] Adinolfi S, Patinen T, Jawahar Deen A, Pitkänen S, Härkönen J, Kansanen E, *et al*. The KEAP1-NRF2 pathway: Targets for therapy and role in cancer. Redox Biology. 2023; 63: 102726. https://doi.org/10.1016/j.redox.2023.102726.

[10] Guo Z, Mo Z. Keap1-Nrf2 signaling pathway in angiogenesis and vascular diseases. Journal of Tissue Engineering and Regenerative Medicine. 2020; 14: 869–883. https://doi.org/10.1002/term.3053.

[11] Uruno A, Yamamoto M. The KEAP1-NRF2 System and Neurodegenerative Diseases. Antioxidants & Redox Signaling. 2023; 38: 974–988. https://doi.org/10.1089/ars.2023.0234.

[12] Shekh-Ahmad T, Eckel R, Dayalan Naidu S, Higgins M, Yamamoto M, Dinkova-Kostova AT, *et al*. KEAP1 inhibition is neuroprotective and suppresses the development of epilepsy. Brain: a Journal of Neurology. 2018; 141: 1390–1403. https://doi.org/10.1093/brain/awy071.

[13] Manavi MA, Mohammad Jafari R, Shafaroodi H, Dehpour AR. The Keap1/Nrf2/ARE/HO-1 axis in epilepsy: Crosstalk between oxidative stress and neuroinflammation. International Immunopharmacology. 2025; 153: 114304. https://doi.org/10.1016/j.intimp.2025.114304.

[14] Narendra DP, Youle RJ. The role of PINK1-Parkin in mitochondrial quality control. Nature Cell Biology. 2024; 26: 1639–1651. https://doi.org/10.1038/s41556-024-01513-9.

[15] Li J, Yang D, Li Z, Zhao M, Wang D, Sun Z, *et al*. PINK1/Parkin-mediated mitophagy in neurodegenerative diseases. Ageing Research Reviews. 2023; 84: 101817. https://doi.org/10.1016/j.arr.2022.101817.

[16] Jia J, Zhao WM, Wang X, Guo M, Sun J. Triptolide impedes high glucose-induced cell function in HK2 cells through PRKN-mediated ubiquitination of ACSL1. The Journal of Endocrinology. 2025; 267: e250095. https://doi.org/10.1530/JOE-25-0095.

[17] Kalinski AL, Kar AN, Craver J, Tosolini AP, Sleigh JN, Lee SJ, *et al*. Deacetylation of Miro1 by HDAC6 blocks mitochondrial transport and mediates axon growth inhibition. The Journal of Cell Biology. 2019; 218: 1871–1890. https://doi.org/10.1083/jcb.201702187.

[18] Srivastava A, Banerjee J, Dubey V, Tripathi M, Chandra PS, Sharma MC, *et al*. Role of Altered Expression, Activity and Subcellular Distribution of Various Histone Deacetylases (HDACs) in Mesial Temporal Lobe Epilepsy with Hippocampal Sclerosis. Cellular and Molecular Neurobiology. 2022; 42: 1049–1064. https://doi.org/10.1007/s10571-020-00994-0.

[19] Loi M, Gennaccaro L, Fuchs C, Trazzi S, Medici G, Galvani G, *et al*. Treatment with a GSK-3β/HDAC Dual Inhibitor Restores Neuronal Survival and Maturation in an In Vitro and In Vivo Model of *CDKL5* Deficiency Disorder. International Journal of Molecular Sciences. 2021; 22: 5950. https://doi.org/10.3390/ijms22115950.

[20] Lu Z, Jiang Z, Huang X, Chen Y, Feng L, Mai J, *et al*. Anti-Alzheimer effects of an HDAC6 inhibitor, WY118, alone and in combination of lithium chloride: Synergistic suppression of ferroptosis via the modulation of tau phosphorylation and MAPK signaling. European Journal of Pharmacology. 2025; 997: 177605. https://doi.org/10.1016/j.ejphar.2025.177605.

[21] San Y, Wang M. Cordycepin Ameliorates Kainic Acid-Induced HT22 Cell Neurotoxicity by Activating GPR120-Mediated Mitophagy. Developmental Neurobiology. 2025; 85: e22961. https://doi.org/10.1002/dneu.22961.

[22] Sheng YC, Huang JN, Wu WL, Wan XR, Wang J, Qin ZH, *et al*. TIGAR plays neuroprotective roles in MPP^+/MPTP-induced Parkinson's disease by alleviating ferroptosis. European Journal of Pharmacology. 2025; 995: 177430. https://doi.org/10.1016/j.ejphar.2025.177430.

[23] Wang C, Chen S, Guo H, Jiang H, Liu H, Fu H, *et al*. Forsythoside A Mitigates Alzheimer's-like Pathology by Inhibiting Ferroptosis-mediated Neuroinflammation via Nrf2/GPX4 Axis Activation. International Journal of Biological Sciences. 2022; 18: 2075–2090. https://doi.org/10.7150/ijbs.69714.

[24] Yagnik D, Hills F. Urate crystals induce macrophage PAF AH secretion which is differentially regulated by TGFβ1 and hydrocortisone. Molecular Medicine Reports. 2018; 18: 3506–3512. https://doi.org/10.3892/mmr.2018.9323.

[25] Xu S, Zheng Q, Chen C, Wang Z, Liu G. BMP6 ubiquitination mediated by SMURF1 suppresses ferroptosis and diminishes sensitivity to doxorubicin in gastric cancer. Gastroenterology Report. 2025; 13: goaf051. https://doi.org/10.1093/gastro/goaf051.

[26] Feng F, Luo R, Mu D, Cai Q. Ferroptosis and Pyroptosis in Epilepsy. Molecular Neurobiology. 2024; 61: 7354–7368. https://doi.org/10.1007/s12035-024-04018-6.

[27] Liu Y, Tao S, Liao L, Li Y, Li H, Li Z, *et al*. TRIM25 promotes the cell survival and growth of hepatocellular carcinoma through targeting Keap1-Nrf2 pathway. Nature Communications. 2020; 11: 348. https://doi.org/10.1038/s41467-019-14190-2.

[28] Tong G, Chen Y, Chen X, Fan J, Zhu K, Hu Z, *et al*. FGF18 alleviates hepatic ischemia-reperfusion injury via the USP16-mediated KEAP1/Nrf2 signaling pathway in male mice. Nature Communications. 2023; 14: 6107. https://doi.org/10.1038/s41467-023-41800-x.

[29] Wang H, Ye J, Peng Y, Ma W, Chen H, Sun H, *et al*. CKLF induces microglial activation via triggering defective mitophagy and mitochondrial dysfunction. Autophagy. 2024; 20: 590–613. https://doi.org/10.1080/15548627.2023.2276639.

[30] Wu X, Zheng Y, Liu M, Li Y, Ma S, Tang W, *et al*. BNIP3L/NIX degradation leads to mitophagy deficiency in ischemic brains. Autophagy. 2021; 17: 1934–1946. https://doi.org/10.1080/15548627.2020.1802089.

[31] Xie R, Zhao W, Lowe S, Bentley R, Hu G, Mei H, *et al*. Quercetin alleviates kainic acid-induced seizure by inhibiting the Nrf2-mediated ferroptosis pathway. Free Radical Biology & Medicine. 2022; 191: 212–226. https://doi.org/10.1016/j.freeradbiomed.2022.09.001.

[32] Luo X, Wang Y, Zhu X, Chen Y, Xu B, Bai X, *et al*. MCL attenuates atherosclerosis by suppressing macrophage ferroptosis via targeting KEAP1/NRF2 interaction. Redox Biology. 2024; 69: 102987. https://doi.org/10.1016/j.redox.2023.102987.

[33] Bellezza I, Giambanco I, Minelli A, Donato R. Nrf2-Keap1 signaling in oxidative and reductive stress. Biochimica et Biophysica Acta. Molecular Cell Research. 2018; 1865: 721–733. https://doi.org/10.1016/j.bbamcr.2018.02.010.

[34] Fikry H, Saleh LA, Mahmoud FA, Gawad SA, Abd-Alkhalek HA. CoQ10 targeted hippocampal ferroptosis in a status epilepticus rat model. Cell and Tissue Research. 2024; 396: 371–397. https://doi.org/10.1007/s00441-024-03880-z.

[35] Ye Q, Zeng C, Dong L, Wu Y, Huang Q, Wu Y. Inhibition of ferroptosis processes ameliorates cognitive impairment in kainic acid-induced temporal lobe epilepsy in rats. American Journal of Translational Research. 2019; 11: 875–884.

[36] An W, Xing M, Fan W, Zheng K, Xu X. The ketogenic diet al-

leviates neuronal ferroptosis in epilepsy via HDAC4/TFRC signalling. Archives of Medical Science. 2025. https://doi.org/10.5114/aoms/207708.

[37] Li J, Lu K, Sun F, Tan S, Zhang X, Sheng W, *et al*. Panaxydol attenuates ferroptosis against LPS-induced acute lung injury in mice by Keap1-Nrf2/HO-1 pathway. Journal of Translational Medicine. 2021; 19: 96. https://doi.org/10.1186/s12967-021-02745-1.

[38] Kishore M, Pradeep M, Narne P, Jayalakshmi S, Panigrahi M, Patil A, *et al*. Regulation of Keap1-Nrf2 axis in temporal lobe epilepsy-hippocampal sclerosis patients may limit the seizure outcomes. Neurological Sciences: Official Journal of the Italian Neurological Society and of the Italian Society of Clinical Neurophysiology. 2023; 44: 4441–4450. https://doi.org/10.1007/s10072-023-06936-0.

[39] Wang D, Cui Y, Gao F, Zheng W, Li J, Xian Z. Keap1/Nrf2 signaling pathway participating in the progression of epilepsy via regulation of oxidative stress and ferroptosis in neurons. Clinics (Sao Paulo, Brazil). 2024; 79: 100372. https://doi.org/10.1016/j.clinsp.2024.100372.

[40] Zhang XW, Feng N, Liu YC, Guo Q, Wang JK, Bai YZ, *et al*. Neuroinflammation inhibition by small-molecule targeting USP7 noncatalytic domain for neurodegenerative disease therapy. Science Advances. 2022; 8: eabo0789. https://doi.org/10.1126/sciadv.abo0789.

[41] Wang J, Cao Y, Lu Y, Zhu H, Zhang J, Che J, *et al*. Recent progress and applications of small molecule inhibitors of Keap1-Nrf2 axis for neurodegenerative diseases. European Journal of Medicinal Chemistry. 2024; 264: 115998. https://doi.org/10.1016/j.ejmech.2023.115998.

[42] Chang B, Su Y, Li T, Zheng Y, Yang R, Lu H, *et al*. Mito-TEMPO Ameliorates Sodium Palmitate Induced Ferroptosis in MIN6 Cells through PINK1/Parkin-Mediated Mitophagy. Biomedical and Environmental Sciences: BES. 2024; 37: 1128–1141. https://doi.org/10.3967/bes2024.111.

[43] Clausen L, Okarmus J, Voutsinos V, Meyer M, Lindorff-Larsen K, Hartmann-Petersen R. PRKN-linked familial Parkinson's disease: cellular and molecular mechanisms of disease-linked variants. Cellular and Molecular Life Sciences: CMLS. 2024; 81: 223. https://doi.org/10.1007/s00018-024-05262-8.

[44] Qi Y, Zhang J, Zhang Y, Zhu H, Wang J, Xu X, *et al*. Curcuma wenyujin extract alleviates cognitive deficits and restrains pyroptosis through PINK1/Parkin mediated autophagy in Alzheimer's disease. Phytomedicine: International Journal of Phytotherapy and Phytopharmacology. 2025; 139: 156482. https://doi.org/10.1016/j.phymed.2025.156482.

[45] Zhou X, Yang Y, Tai Z, Zhang H, Yang J, Luo Z, *et al*. The mechanism of mitochondrial autophagy regulating Clathrin-mediated endocytosis in epilepsy. Epilepsia Open. 2024; 9: 1252–1264. https://doi.org/10.1002/epi4.12945.

[46] Mondal P, Bai P, Gomm A, Bakiasi G, Lin CCJ, Wang Y, *et al*. Structure-Based Discovery of A Small Molecule Inhibitor of Histone Deacetylase 6 (HDAC6) that Significantly Reduces Alzheimer's Disease Neuropathology. Advanced Science (Weinheim, Baden-Wurttemberg, Germany). 2024; 11: e2304545. https://doi.org/10.1002/advs.202304545.

[47] Kumar V, Kundu S, Singh A, Singh S. Understanding the Role of Histone Deacetylase and their Inhibitors in Neurodegenerative Disorders: Current Targets and Future Perspective. Current Neuropharmacology. 2022; 20: 158–178. https://doi.org/10.2174/1570159X19666210609160017.

[48] Yuan Y, Zhai Y, Chen J, Xu X, Wang H. Kaempferol Ameliorates Oxygen-Glucose Deprivation/Reoxygenation-Induced Neuronal Ferroptosis by Activating Nrf2/SLC7A11/GPX4 Axis. Biomolecules. 2021; 11: 923. https://doi.org/10.3390/biom11070923.

[49] Wang H, Wu S, Jiang X, Li W, Li Q, Sun H, *et al*. Acteoside alleviates salsolinol-induced Parkinson's disease by inhibiting ferroptosis via activating Nrf2/SLC7A11/GPX4 pathway. Experimental Neurology. 2025; 385: 115084. https://doi.org/10.1016/j.expneurol.2024.115084.

[50] Jiang X, Stockwell BR, Conrad M. Ferroptosis: mechanisms, biology and role in disease. Nature Reviews. Molecular Cell Biology. 2021; 22: 266–282. https://doi.org/10.1038/s41580-020-00324-8.